PROCESSING OF CENOSPHERE-CEMENT/ASPHALT COMPOSITE MATERIALS AND EVALUATION OF THEIR MECHANICAL AND ACOUSTIC PROPERTIES

Arijit Bose and Arun Shukla
University of Rhode Island

April 2004

URITC PROJECT NO. 536160

PREPARED FOR

UNIVERSITY OF RHODE ISLAND
TRANSPORTATION CENTER

1. Report No	2. Government Accession No.	3. Recipient's Catalog No.
URITC FY01-10	N/A	N/A

4. Title and Subtitle	5. Report Date
Processing of Cenosphere-Cement/Asphalt Composite Materials and Evaluation of their Mechanical and Acoustic Properties	04/09/2004
	6. Performing Organization Code N/A

7. Authors(s)	8. Performing Organization Report No.
Arijit Bose, Arun Shukla	N/A

9. Performing Organization Name and Address	10. Work Unit No. (TRAIS)
University of Rhode Island, Dept. of Chemical Engineering, 217 Crawford Hall, Kingston, RI 02881 (401) 874- 2804 bosea@egr.uri.edu	N/A
	11. Contract or Grant No. URI 536160
	13. Type of Report and Period Covered Final

12. Sponsoring Agency Name and Address	14. Sponsoring Agency Code
University of Rhode Island Transportation Center 85 Briar Lane Kingston, RI 02881	A study conducted in cooperation with U.S. DOT

15. Supplementary Notes

N/A

16. Abstract

Cenospheres are hollow, aluminum silicate spheres, between 10–300μm in diameter. Their low specific gravity (0.67) make them ideal replacements for fine sand for producing low density concrete. In this research, the moisture uptake and loss by cenospheres, and water uptake and loss in cenosphere/concrete composites have been studied. The equilibrium moisture content of cenospheres exposed to air of 85% relative humidity is 0.15 kg moisture / kg dry cenospheres. This moisture content is about 18 times higher than that of sand, reflecting the porous nature of cenospheres. The temporal evolution of water penetration into the cenosphere/concrete is modeled using Washburn kinetics. The effective pore size using this model is of the order of several nanometers. The results imply a lack of connectivity within the pores, leading to a low permeability. SEM images of the concrete reveal pore sizes of the order of 2-5μm. When the 'wet' cenospheres are exposed to air of 20% relative humidity at room temperature the drying flux shows a classical behavior – a constant rate followed by a linear falling rate period. Thus experiments done at these conditions can be used to predict drying times for wet cenospheres exposed to other environments. The drying of saturated cenosphere/concrete and the normal concrete material exposed to air at 20% relative humidity is compared at 23°C, 30°C and 40°C. The flux of water vapor away from both the cenosphere/concrete as well as the normal concrete shows a non-linear change with moisture content throughout the drying cycle, implying that the pore structure within the concrete strongly influences the drying behavior.

The acoustic behavior of different grades of cenosphere rich concrete has also been investigated experimentally. Properties such as absorption coefficient, reflection coefficient and acoustic impedance and their dependence on frequency have been measured. The effect of cenospheres on the acoustic properties including the complete acoustic frequency response characteristic of cenosphere rich concrete is reported.

17. Key Words	18. Distribution Statement
Cenospheres, concrete, acoustic, moisture migration	No restrictions. This document is available to the Public through the URI Transportation Center, 85 Briar Lane, Kingston, RI 02881

19. Security Classif. (of this report)	20. Security Classif. (of this page)	21. No. of Pages	22. Price
Unclassified	Unclassified	**27**	N/A

Form DOT F 1700.7 (8-72) Reproduction of completed page authorized (art. 5/94)

Table of Contents

List of Figures

1. Moisture Migration

1.1 Introduction

Cenospheres are hollow aluminum silicate micro-spheres obtained from the fly ash of coal fired thermal power plants. Their diameters vary from 10 to 300 μm with a typical wall thickness of about 5-10% of the diameter. Figure 1(a) and (b) show SEM images of cenospheres, clearly showing their size, hollow nature and their porosity. They have a specific gravity of 0.67 and a bulk density of 375 kg/m^3. Their chemical composition is primarily silica (65%) and alumina (30%) with trace amount of oxides of Fe, Ca, K and Ti. As a constituent in composite materials, these cenospheres have enormous potential to reduce density, provide better insulation, improve impact resistance and reduce shrinkage and warpage (Berry *et al.*, 1986, Rohatgi *et al.*, 1995 and Wandell, 1996). Coal fired power plants produce abundant quantities of these spheres (as high as 40 million tons per plant per year), which are normally disposed of in landfills. Their spherical morphology, chemical characteristics, structure as well as their mechanical and energy-attenuating properties can be exploited synergistically with those of cement to form lightweight materials suitable for bridge decks, pavements and highways.

(1a)

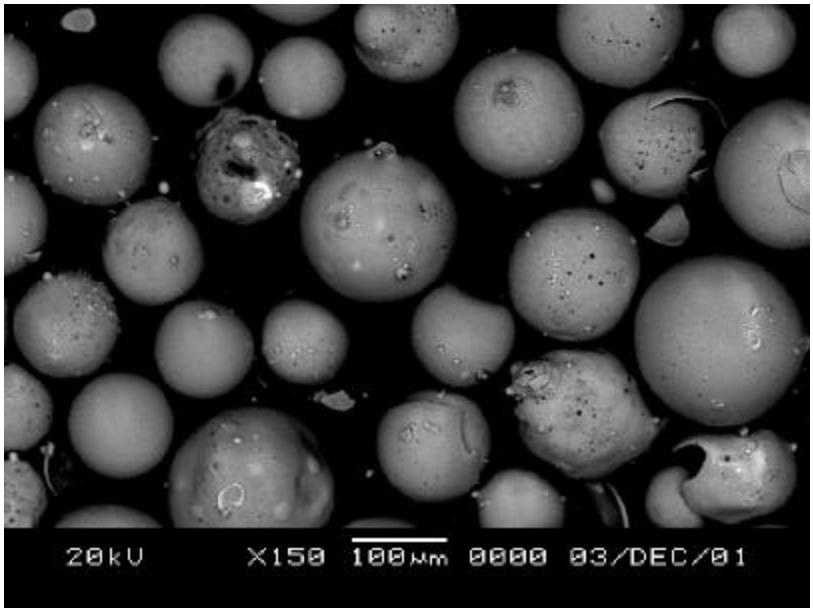

(1b)

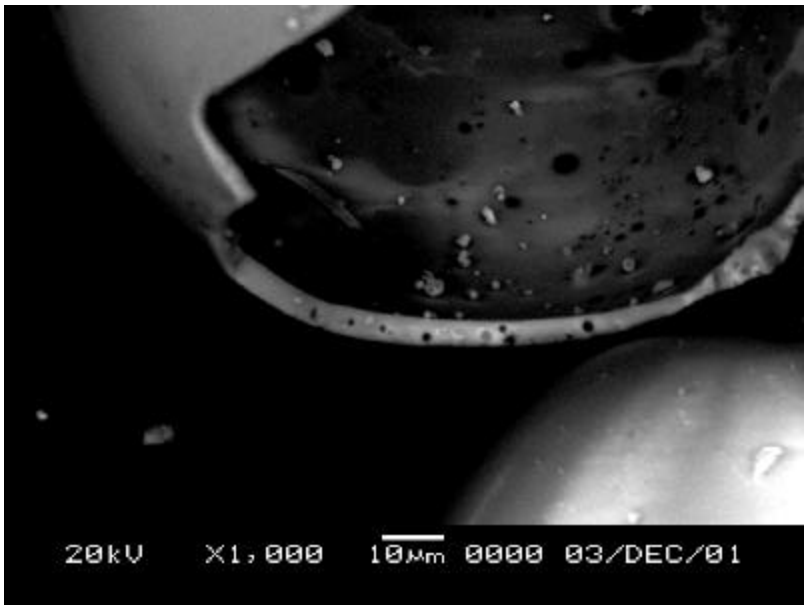

Figure 1: SEM Micrograph of the cenospheres indicating the porous inner/outer surfaces and the porous thin walls of a broken cenosphere

The water content in concrete has a significant impact on its mechanical properties. When cenospheres are used to replace the fine aggregates in concrete, the inherent differences in the equilibrium moisture content require different amounts of water to be added prior to curing the concrete. In the first set of experiments reported here, the equilibrium moisture contents, as well as the kinetics of water vapor uptake and drying of cenospheres is compared to fine sand. Thus these experiments provide a useful metric for sample preparation since they quantify the amount of water bound to the cenospheres and therefore not available for the cement.

An important factor that impacts the durability of concrete is the uptake and loss of water. Ingress of water in the concrete provides a path for the transport of deleterious materials such as chloride and sulfate ions. This leads to corrosion of reinforcement bars, and substantial deterioration in the mechanical properties and service life of the concrete. The penetration of water in the concrete through its pores can also lead to undesirable cracking during freezing. The second set of experiments is geared towards monitoring and comparing water penetration in cenosphere/concrete and normal concrete.

Concrete used in structural applications is often exposed to environments that can be extremely dry. Under those conditions, it is important to understand the rate of loss of water. In the third set of experiments, moisture loss in cenosphere-concrete composites are monitored at 23°C, 30C and 40C using air of 20% relative humidity.

1.2 Materials and Methods

1.2.1 Moisture uptake

Cenospheres and sand samples weighing 1.63g and 3.50g (each sample had the same volume) respectively were exposed to a constant temperature (23°C), constant relative humidity (85%) environment inside a closed chamber. The moisture uptake in the samples was monitored over time by measuring the mass of the samples at regular intervals. A plot of the fractional weight gain (weight of water absorbed/dry weight of sample) over time for the cenospheres and sand samples is shown in Figure 2.

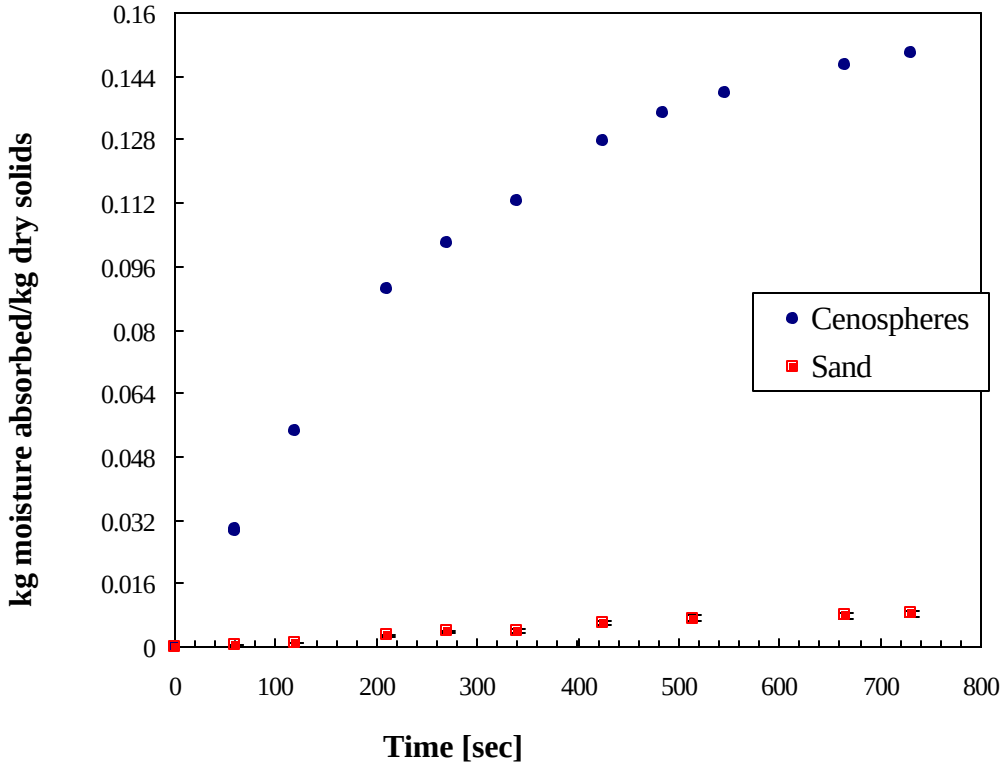

Figure 2: Fractional weight gain versus time for the cenospheres and sand.

The equilibrium moisture content of cenospheres exposed to air of 85% relative humidity is 0.15 kg water/kg dry cenospheres. For sand, this number is 0.0084 kg water/kg dry solid. This 18-fold difference in the moisture absorption capacity is caused by the porous nature of cenospheres.

1.2.2 Preparation of cenosphere/concrete sample for water influx

The concrete test specimen was prepared according to the ASTM standard C 192. The specimens were disks of diameter 0.1m and thickness 0.025m. The disks were sliced from a cast cylindrical specimen of dimensions diameter 0.1m and height 0.2m. They were dried at 50^{o}C to achieve a constant weight and then exposed to water in a bath, as shown in Figure 3. Water penetration from the curved surface was eliminated by tightly covering those edges with an impermeable plastic sheet. The mass of the specimen was measured using an electronic balance with a resolution of 1g at regular intervals. The weight gain by the specimens is calculated and is normalized by the initial dry weight of the sample.

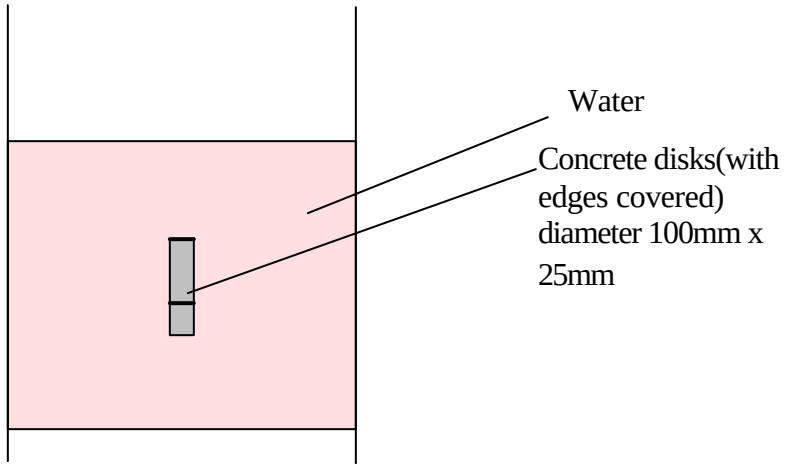

Figure 3: Schematic of the experimental set-up for penetration of water in the concrete

1.2.3 Absorption of water

The material properties of concrete depend on the mix design, preparation and environmental conditions (Martys *et al.1997)*. Thus the concrete properties are highly variable. The normalized weight gain in the concrete samples is plotted versus time in Figure 4. Note that water uptake in both the samples is extremely slow, showing saturation after approximately 4 days. Over the first two hours the water absorption profiles for the normal and cenosphere-concrete are very similar when seen at this scale. However, the equilibrium moisture content for the lightweight concrete is 1.16×10^{-2} kg water/kg dry concrete, more than the equilibrium moisture content of 9.425×10^{-3} kg water/kg dry concrete for the normal concrete

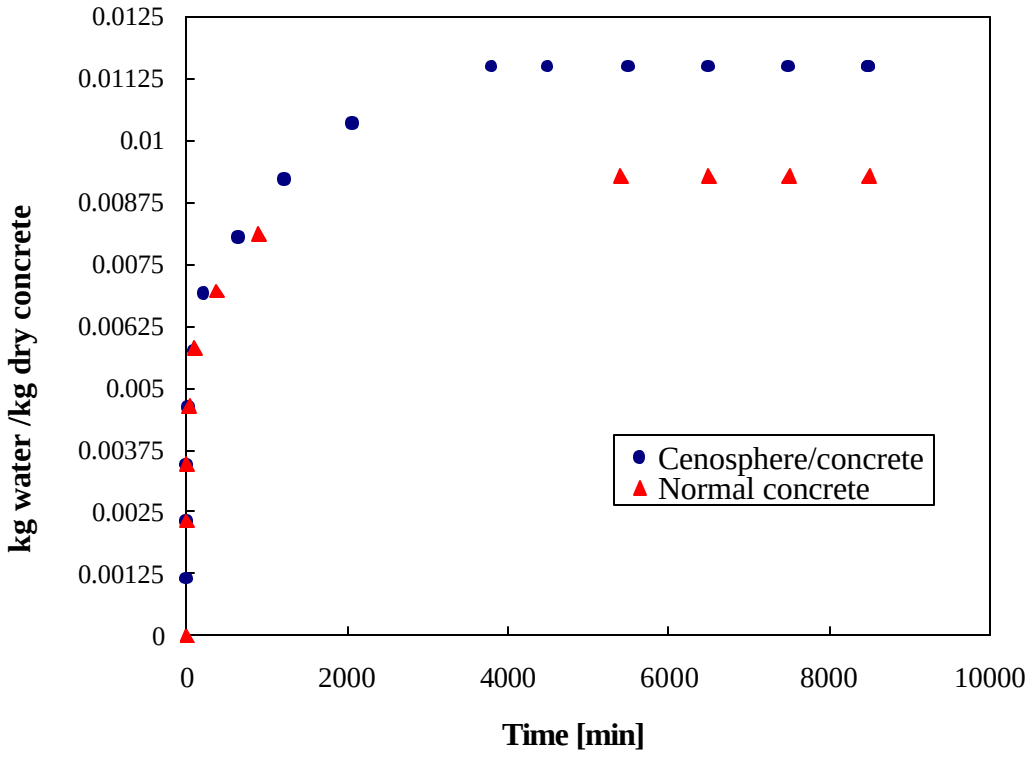

Figure 4: Fractional weight gain versus time for the cenosphere/concrete and normal concrete samples

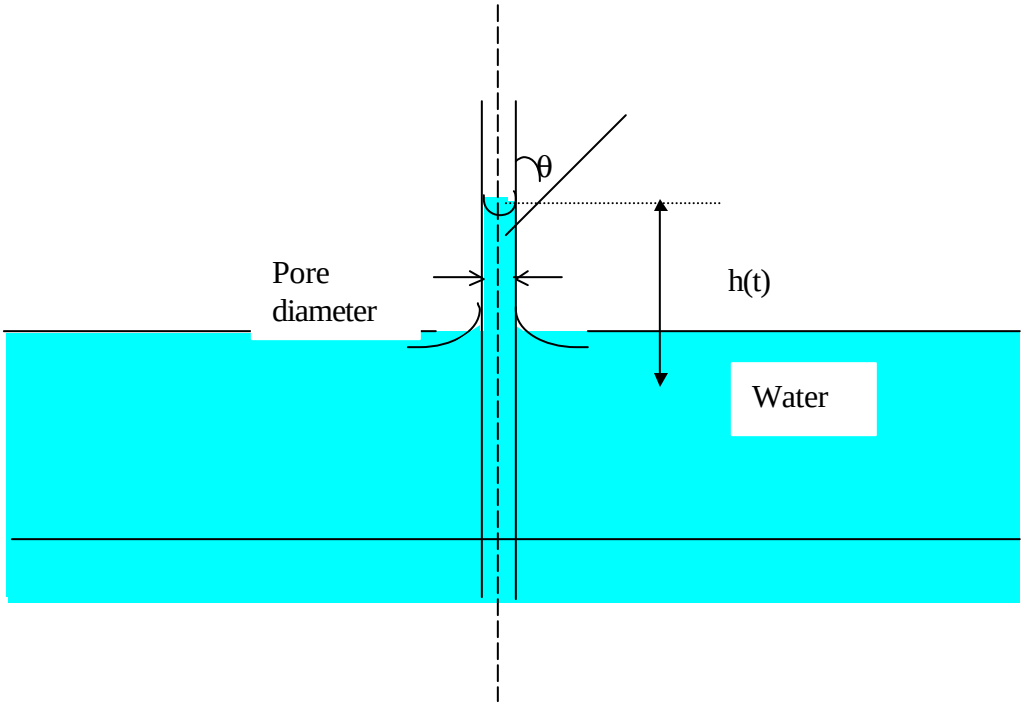

Figure 5: Forces acting on water transport due to capillary rise in concrete pore

Since the water penetration is driven by capillary transport in a porous medium like concrete, this process is modeled using Washburn kinetics, and an effective pore diameter is obtained using the analysis below.

Neglecting inertia, the instantaneous force balance on a slug of liquid rising in a cylindrical pore is (see Figure 5)

$$2\pi r_c \gamma \cos\theta - 2\pi r_c \tau h(t) - \pi r_c^2 h(t) \rho g = 0 \qquad (1)$$

where r_c is the effective pore radius, γ is the surface tension of water (72×10^{-3} N/m at 23°C), θ is the wetting angle, τ is the viscous shear stress acting on the fluid at the wall and h(t) is the liquid penetration depth. Since the experiments were performed with water absorption from the lateral faces of the sample, gravity can be neglected.
Assuming that the flow in the pore is fully developed, the viscous shear stress for a Newtonian liquid is:

$$\tau = \frac{4\mu}{r_c} V = \frac{4\mu}{r_c} \frac{dh}{dt} \qquad (2)$$

Substituting Eq.(2) into Eq.(1), and rearranging the terms,

$$h = \sqrt{\frac{r_c g \cos\theta}{2}} t = S\, t^{1/2} \qquad (3)$$

where S is the sorptivity for concrete.

The penetration depth 'h(t)' is obtained from the experimental measurement of weight gain $\Delta W(t)$, from

$$\Delta W(t) = 2\, h(t)\, A\, \rho\, \varepsilon \qquad (4)$$

Here A is the area of cross section, ρ is density of water and ε is the porosity of the concrete.

ε is calculated using the data for the actual volume of the concrete and the summation of volume of the components in the mix design for the concrete.

Thus,

$$\varepsilon = 1 - \left[\frac{\text{Actual volume of concrete sample}}{\text{Sum of volumes of the individual components in the concrete mix}} \right] \qquad (5)$$

Since the sample is completely dried prior to the water influx experiments, the water volume is neglected for calculating ε. $\varepsilon = 0.071$ and 0.063 for the normal and cenosphere/concrete respectively.

If Washburn kinetics is obeyed, a plot of h versus $t^{1/2}$ should be linear. Figure 6(a) shows that this relationship is valid at short times, but not past 10 min. The effective pore sizes are 0.6×10^{-9} m for cenosphere/concrete and 2.2×10^{-9} m for normal concrete.

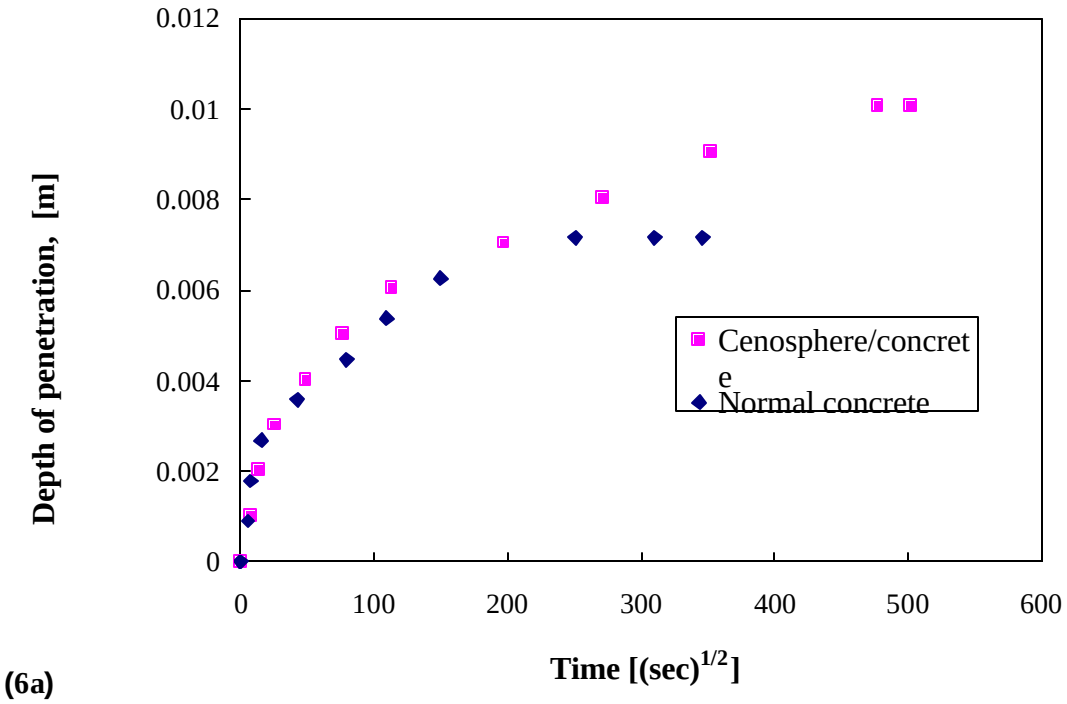

(6a)

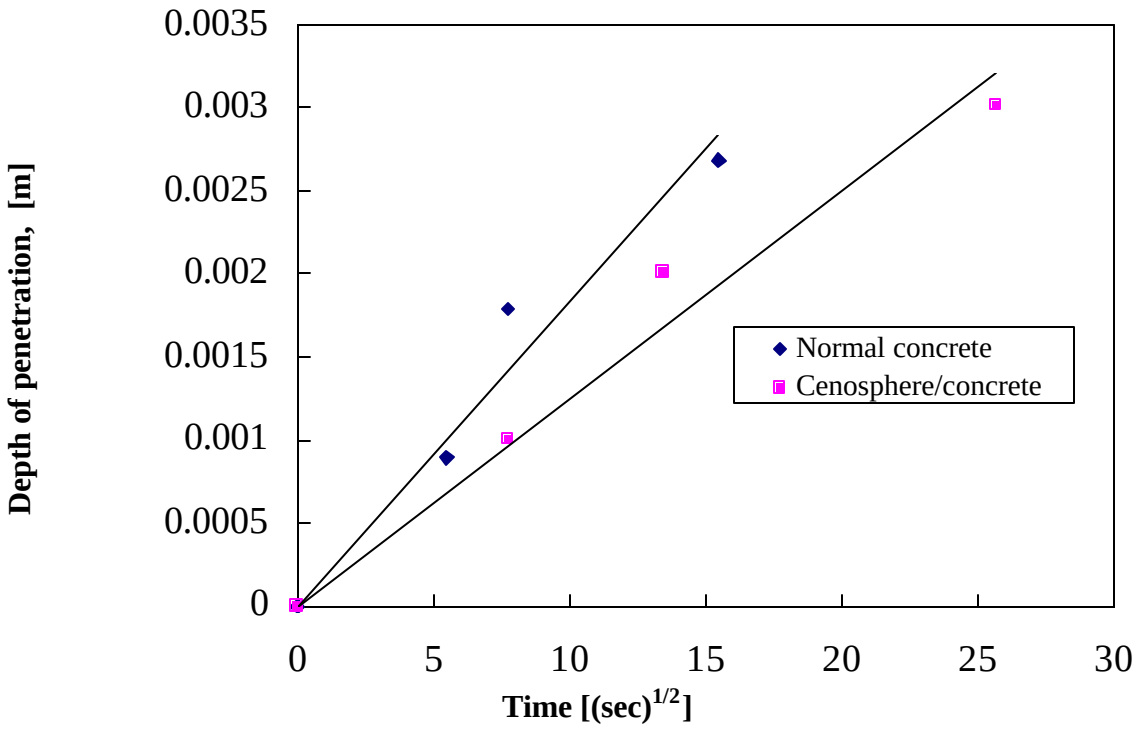

(6b)

Figure 6**:** The variation of h with time and initial weight gain dependence on $t^{1/2}$

A SEM image of a polished cenosphere/concrete is shown in Figure 7. While the pore size varies widely, it is of the order of 0.5μm, and is not of the order of 10^{-9}m as predicted from the Washburn equation. This is a clear indication that the pores in the concrete are blocked, leading to the low permability. The deviation from linearity in the Washburn plots over longer time scales is an artifact of the experimental method, where water-fronts approach each other from both right and left. This increases the air pressure within the pockets, and slows down water transport.

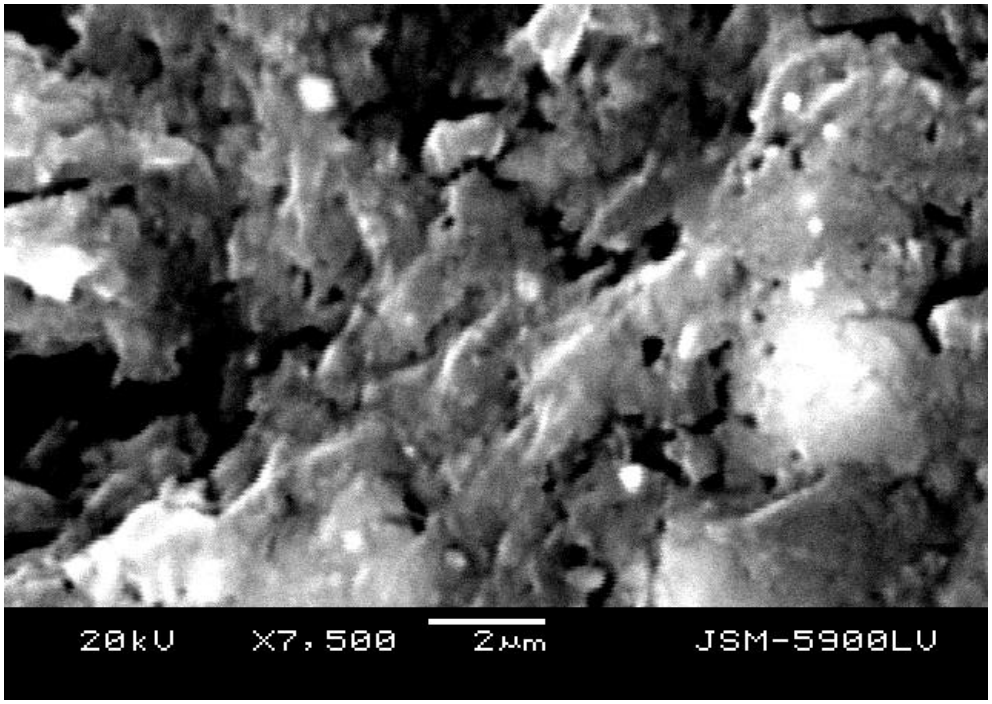

Figure 7: SEM image of the polished concrete surface indicating the actual pore size

1.2.4 Drying of cenospheres and cenosphere/concrete

The cenospheres sample used to study the moisture uptake was allowed to desorb by exposure to dry environment at a low relative humidity (20%) at room temperature of 23°C. Characteristic drying curves for the cenospheres are seen in Figures 8 (a) and (b). As shown in Figure 8(b), a classical drying curve is obtained – a constant rate period followed by a falling rate period until the sample is dry. Experiments done at these conditions can then be used to predict drying behavior in completely different conditions by adjusting for the new mass transfer coefficient and driving force in the new environment.

Drying experiments were performed for saturated cenosphere/concrete and the normal concrete at three different temperatures, 23°C, 30°C and 40°C. The data are shown in Figures 9 (a) and (b). Unlike the drying results from the cenospheres alone, the water vapor flux from the cenosphere/concrete as well as the normal concrete shows a highly non-linear behavior throughout the drying cycle for all temperatures. (Figure 10). Transport of water vapor through the tortuous pores of concrete control the rate of moisture migration to the surface, leading to this observed complex behavior.

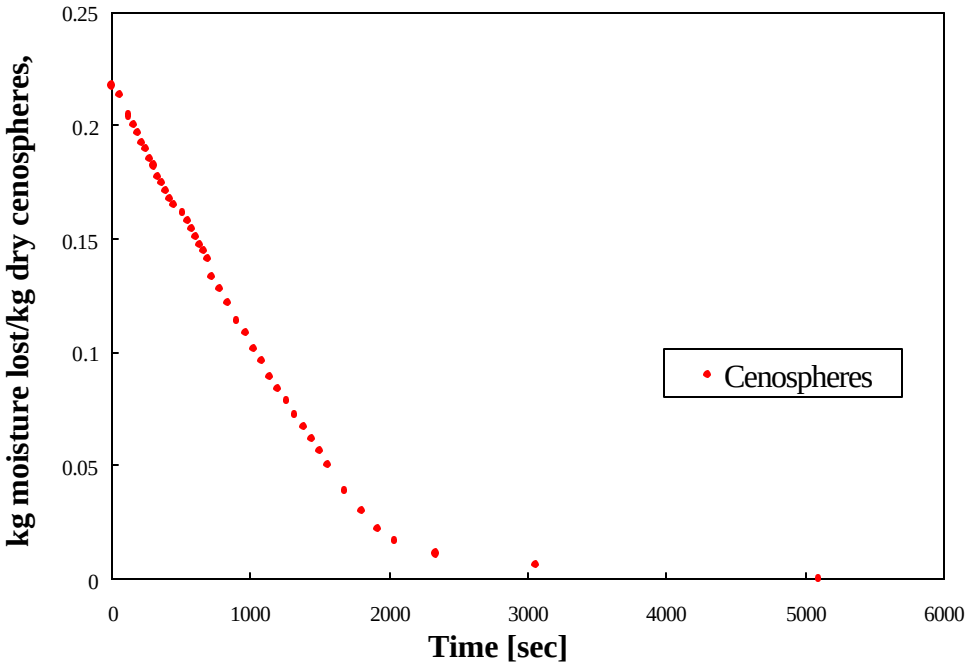

(8a)

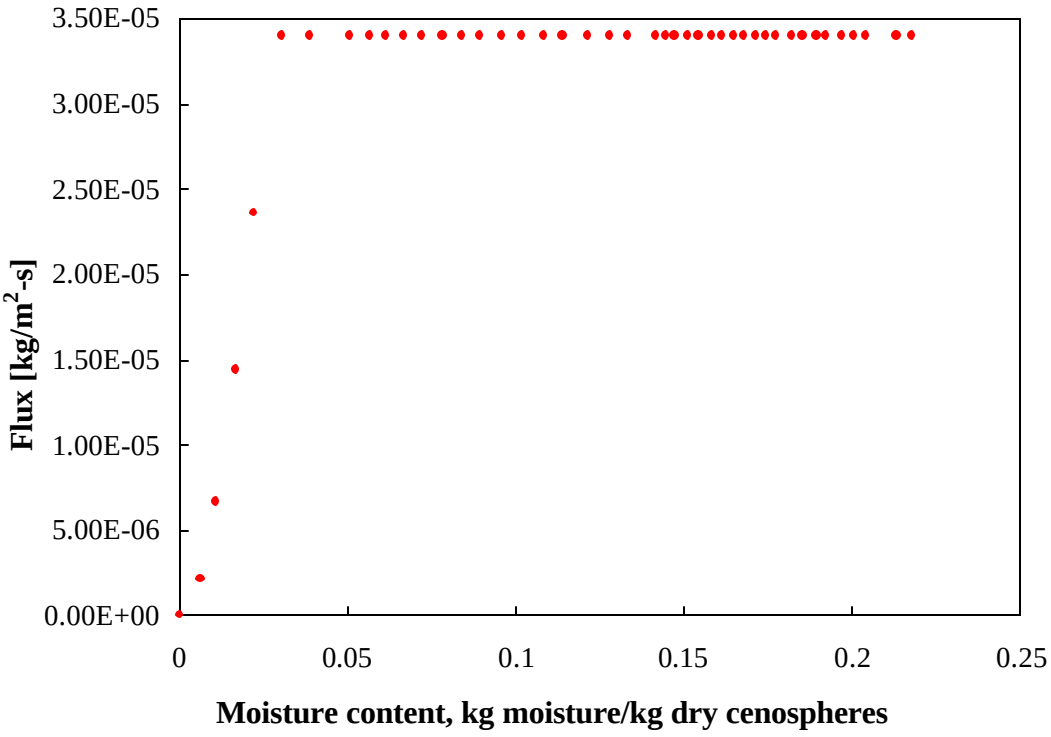

(8b)

Figure 8 (a): Moisture content Vs time for drying of cenospheres at 23°C and RH<50%; 8 (b): Flux Vs Moisture content

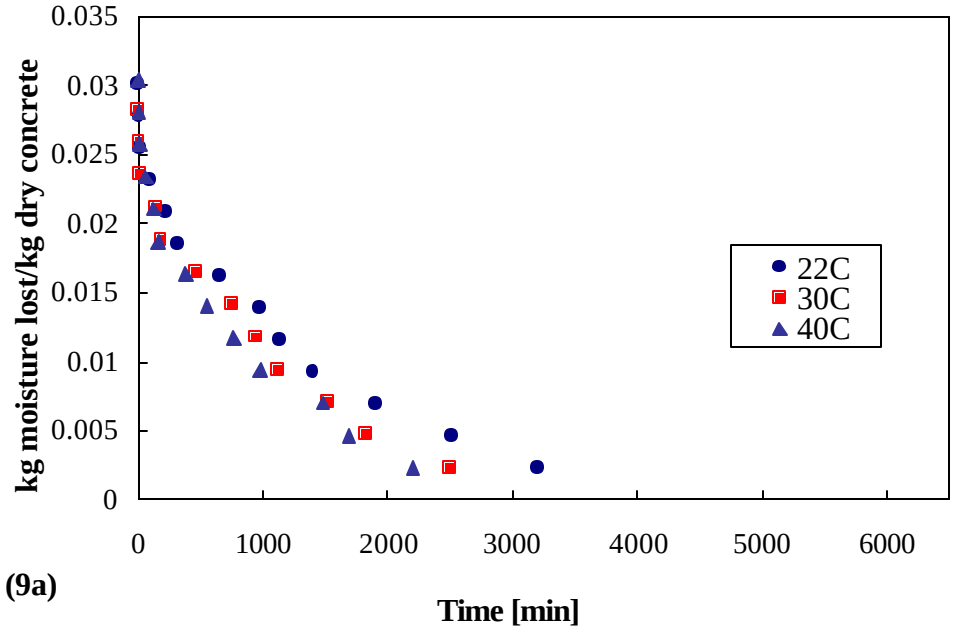

(9a)

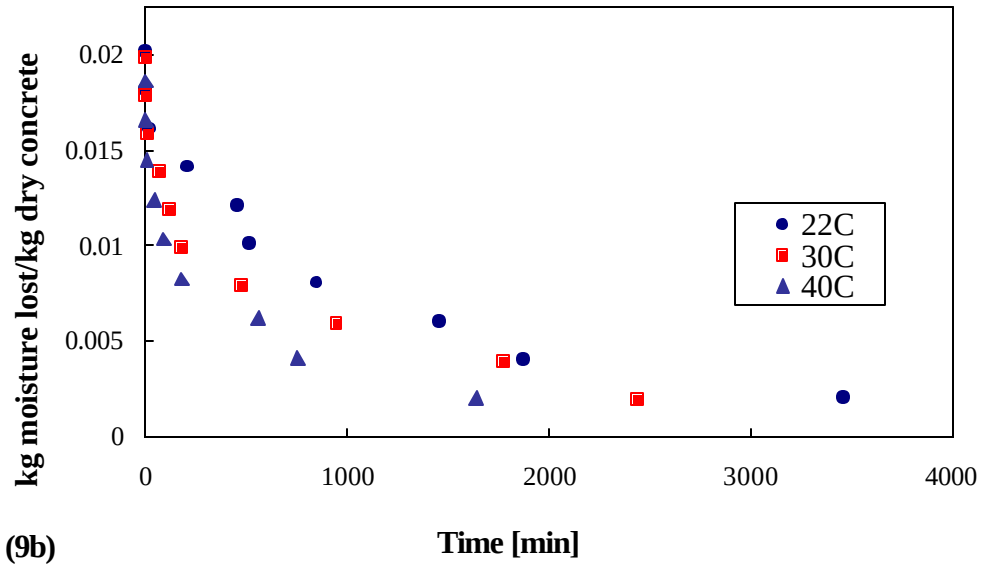

(9b)

Figure 9 (a):Moisture content Vs time for drying of cenosphere/concrete at 23°C,30°C,40°C and RH<50%; 9 (b):Moisture content Vs time for drying of normal concrete at 23°C,30°C,40°C and RH<50%,

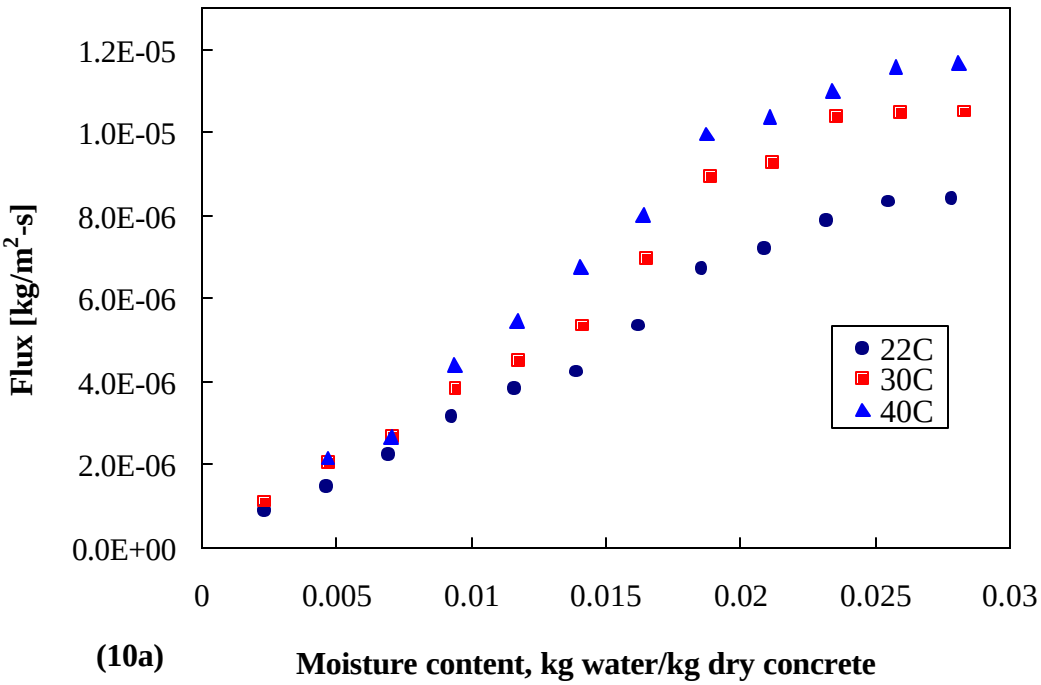

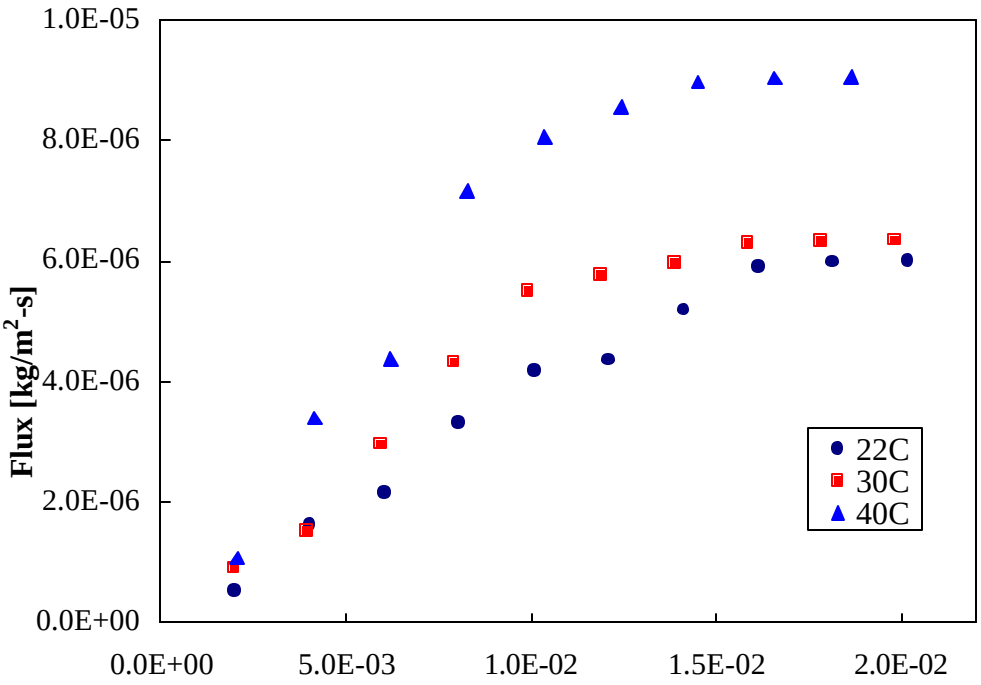

Figure 10 (a): Flux Vs Moisture content – cenosphere/concrete; 10 (b): Flux Vs Moisture content – normal concrete

1.3 Conclusion

Detailed experiments monitoring the moisture uptake and loss in cenospheres, sand and normal as well as cenosphere/concrete samples are undertaken. The moisture uptake by cenospheres is significantly more than the sand. The initial rate of water penetration into concrete shows a characteristic $t^{1/2}$ dependence. The effective pore size for normal concrete is more than the lightweight cenosphere-concrete. The magnitudes of the pore sizes for both the concretes indicates that the rate of water penetration in the porous media is very slow. The lightweight cenosphere/concrete has a higher equilibrium moisture content than the normal concrete. the drying of the normal concrete is faster than the cenosphere/concrete.

ACKNOWLEDGEMENTS

Financial support from the URI Transportation Research Center and the Rhode Island Department of Transportation is gratefully acknowledged.

References

Rohatgi, P.K., R.Q. Guo, B. N. Keshavram, and D. Golden., "Cast aluminium, fly ash composites for engineering applications", *Transactions of the American foundrymen's Society*, number 103, (1995), p.575

Wandell T., "Cenospheres: From waste to profits", The American Ceramic Bulletin, 75:6 (1996), p. 79-81.

Berry, E. E., R. T. Hemmings, and J. Leidner, "Investigation of some new spherical fillers", Plastics Compounding, volume 9 number 7, November-December (1986), p.12.

Martys, N. S, C.F. Ferraris, "Capillary Transport in Mortars and Concrete", Cement and Concrete Research. Volume 27 (1997) p. 747-760

Bentz D. P., M. A. Ehlen, C.F. Ferraris,E.J.Garboczi 7th International Conference on Concrete Pavements; Volume 1. International Society for concrete Pavements. Sept 9-12, 2001, p. 181-193.

Lilkov V., N. Djabarov, G. Bechev, and K. Kolev, "Properties and hydration products of lightweight and expansive cements Part I : Physical and Mechanical properties" , Cement and Concrete Research. Volume 29 (1999) p. 1635-1640.

Kolay P. K.and D. N. Singh, "Physical, chemical, mineralogical, thermal properties of cenospheres from an ash lagoon", Cement and Concrete Research. Volume 31(2001) p. 539-542.

2. Acoustic Properties

2.1 Introduction

Absorption characteristics of different materials have been studied for a long time. Though a wide variety of sound absorbing materials are available, there is need for material which can be used universally without the limitation of use and in an environmentally friendly manner. Cenosphere (ceramic microballoons) rich concrete has been recently tested in the Mechanical Engineering Department of University of Rhode Island. It has shown promising results, from a mechanical perspective. Here we study acoustic properties of this cenosphere filled material to determine if it can be used as sound barrier near highways and other roadways. Its effect on sound absorption properties of asphalt is also matter of intrest.

As it is standard for acoustic characterization, properties such as absorption coefficient, Reflection coefficient and acoustic impedance of the samples are determined and their variation with frequency is studied.

2.2 Review of Previous Work

A number of techniques have been employed to study the acoustic characteristics of different materials they include standing wave method, Transfer function method [1], one microphone technique and Protruding tube method [2]. These techniques are compared with each other [3] and found out to be giving matching results. Related work on sound absorption mechanisms of porous asphalt pavement was done by Yamaguchi et al. [4]; Meiarashi et al. [5]; and Watts et al. [6][7]. Yamaguchi at al. studied absorption properties of asphalt as a function of density, pore size and thickness for different frequencies. Meiarashi et al. analyzed the relationship between noise reduction and the thickness and aggregate size of the drainage asphalt road surface. Watts' work is directed towards porous asphalt surface and noise barriers. He used Boundry Element Method (BEM) approach to determine the extent to which the noise reducing benefits of asphalt could be added to the screening effects of noise barriers in order to obtain the overall reduction in noise levels.

2.3 Theoretical Considerations

Sound absorbing performance of the material is defined by its sound absorption coefficient μ, the ratio of the unreflected sound intensity at the surface to the incident sound intensity. Sound absorption coefficient varies with frequency and also it is a function of material thickness, density and pore size. Unit of sound absorption is Sabins (***A***), one Sabine is square foot of total absorption. Other acoustic properties include sound reflection coefficient which is a ratio of the amount of total reflected sound intensity to the total incident sound intensity and acoustic impedance which is defined as the ratio of sound pressure acting on the surface of the sample to the associated particle velocity normal to the surface.

The theory behind acoustical measurement can be explained as follows. Consider an acoustic plane wave in the standing wave tube. At a particular position in the tube, the sound pressure due to the incident wave at a particular instant of time is given by

$$p_i = A \cos 2\pi f t \qquad (1)$$

and the sound pressure due to reflected wave at the same point at the same instant of time is given by

$$p_r = B \cos 2\pi f \left(t - \frac{2y}{c} \right) \qquad (2)$$

where

p_i , p_r are sound pressure of the incident and reflected wave in Pa

f is the frequency of excitation in Hz

y is distance of point from sample in m

c is the velocity of sound in the tube in m s^{-1}

t is time in s

The total sound pressure at this point, p_y will therefore be:

$$p_y = p_i + p_r = A \cos 2pft + B\cos 2pf\left(t - \frac{2y}{c}\right) \qquad (3)$$

By applying the addition theorem i.e.

$$\cos(\theta - \phi) = \cos\theta \cdot \cos\phi + \sin\theta \cdot \sin\phi \qquad (4)$$

It can be seen that sound pressure will have a maximum value of $(A+B)\cos 2\pi ft$ when $y=\lambda/2$ and a minimum value when $y=\lambda/4$ where λ =wavelength = c/f. A microphone situated at a distance $\lambda/2$ from the sample will receive an alternating sound pressure of frequency f and amplitude (A+B).

The absorption coefficient of the sample will be then

$$a = 1 - \left(\frac{B}{A}\right)^2 \qquad (5)$$

this equation can be written as

$$\alpha = 1 - r^2 \qquad (6)$$

Using the standing wave apparatus, we can measure the ratio, n, of the maximum to minimum sound pressure in the tube, that is the standing wave ratio:

$$n = \frac{P_{MAX}}{P_{MIN}} \qquad (7)$$

therefore $$n = \frac{A+B}{A-B} \qquad (8)$$

An analogy can be drawn between acoustic standing wave ratio and the standing wave ratio measured in electromagnetic wave guides. Hence

$$\frac{B}{A} = \frac{n-1}{n+1} \tag{9}$$

Therefore the absorption coefficient can be expressed in terms of the standing wave ratio by substituting eq(9) in eq(5) yielding:

$$a = 1 - \left(\frac{n-1}{n+1}\right)^2 \tag{10}$$

2.4 Experimental Procedure

The experimental setup for doing the acoustic studies has been installed as shown in Figure 1. It consists of, B&K standing wave apparatus (Type 4002), Bendix (Advance technology center) Frequency generator 343, Tektronix TDS 3014 four channel phosphor oscilloscope and pre-amplifier with band pass filter. The experimental setup is calibrated by conducting experiments on standard test samples. Comparison of experimental and theoretical values for Aluminum sample can be seen in Fig 2. Small difference can be accounted by sound energy dissipation as sound travels along the tube length and acoustic impedance of air itself.

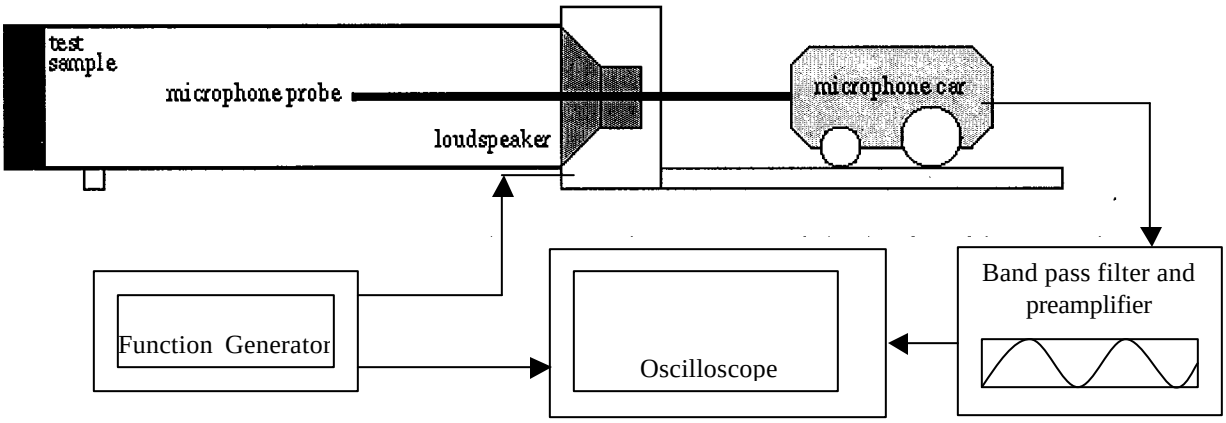

Figure 1: Experimental setup for acoustic studies

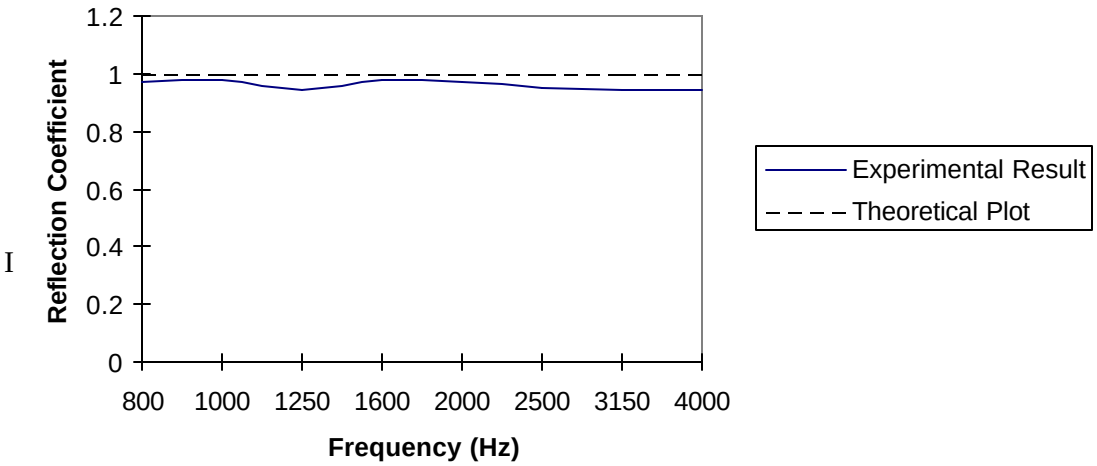

I

Figure 2: Comparing experimental results with theoretical values of Aluminum sample for calibration

In the experimental procedure the test specimen is placed in a specimen holder, fitted at the one end of the impedance tube. A loudspeaker capable of generating the desired frequency is placed at the other end the tube. A microphone is positioned in such a way that it can be moved longitudinally along the tube but remain coaxial with the tube. When the test specimen is placed in the holder the sound levels at the point of maximum and minimum sound intensity can be measured and standing wave ratio can be calculated.

Amplifier and filters are used to clear the noise and record test signals. Using ASTM C384 [8] standards, the absorption coefficient, reflection coefficient and acoustic impedance at a frequency can be determined for the specimen. Specimens of different thickness and size have been examined for the frequency range between 120Hz to 4000Hz, range where human ear is most sensitive to sound.

2.5 Specimen Preparation

Specimens for conducting experiments have been made in the Dynamic Photomechanics Laboratory in Mechanical Engineering Department and Transportation Lab in Civil Engineering Department. Every care has been taken to follow the predetermined standards. About 50 specimens of cenosphere rich cement with different percentage of cenesopheres (from 0 to 70% by volume) and different sizes have been made. For each volume fraction of cenosphere six samples of different (1, 2, and 3 inch long) length and different (3.9 and 1.13 inch) diameter were made. Some of them can be seen in Figure 3. Water to cement ratio was maintained at 0.4 for most of the specimens. At higher percentage of cenospheres, wet cenospheres were used to ensure the proper workability of the resulting mixture. Apart from the specimens for standing wave apparatus, sheets of one square feet dimension with different cenosphere percentage have been made and used for measuring the longitudinal wave velocity for the purpose of calculating acoustic impedance (ρv).

Figure 3: Cement Samples with different percentage of cenospheres

The weight of all the samples was carefully measured to calculate their mass density and it was found that mass density decrease from 1902.7 kg/m^3 for zero percentage cenospheres to 1110.2 for seventy percentage cenosphere as seen in Figure 4.

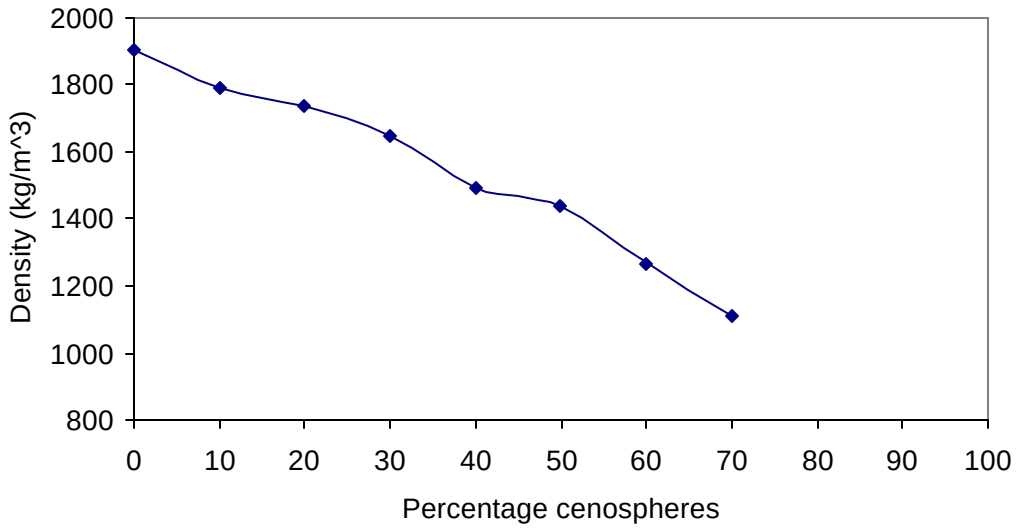

Figure 4: Change in mass density with percentage increase of cenosphers in cement samples.

Asphalt specimens having different cenosphere content have also been made for conducting acoustic experiments. For making the specimens surface course design was used for mixing the fine and coarse aggregate with 6% asphalt by weight. The design for the specimens came from a CAMA software program owned by the Civil Engineering Department in URI. The mineral aggregates were obtained from Cardi in four different sizes. These include both the coarse aggregate; which include the ¾", ½", and the 3/8" size denominations; and the fine aggregate, which was denominated as sand. These material were subjected to sieve analysis, see American Society for Testing Material (ASTM) test C136 [9} or American Association of State Highways and Transportation Officials (AASHTO) test T27. Figure 5 and Figure 6 shows the Result of Sieve analysis for both coarse and fine aggregates respectively.

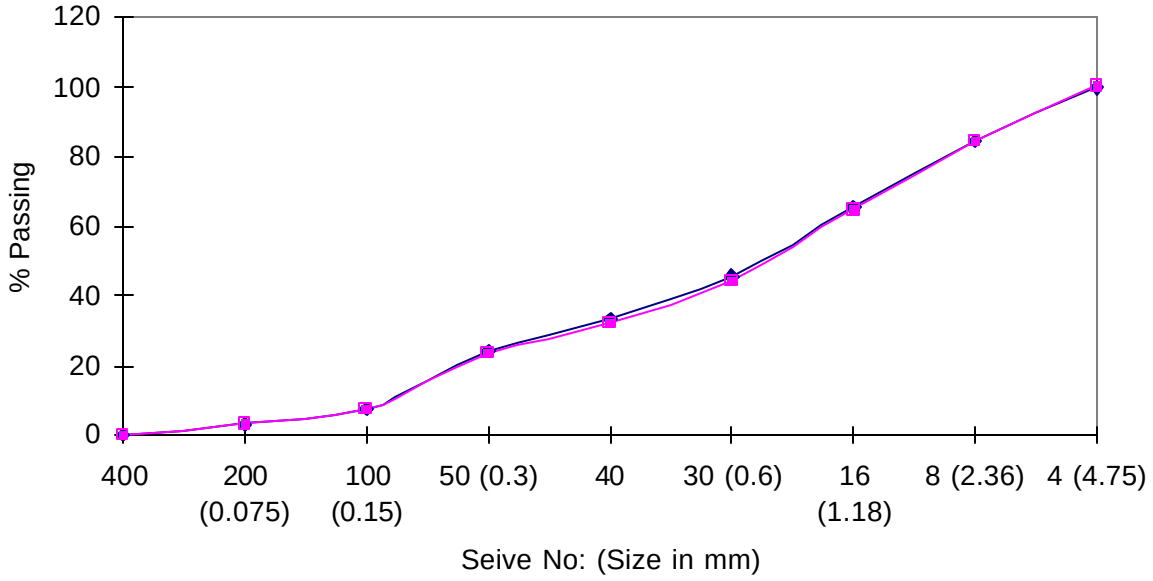

Figure 5: Gradation chart for sand

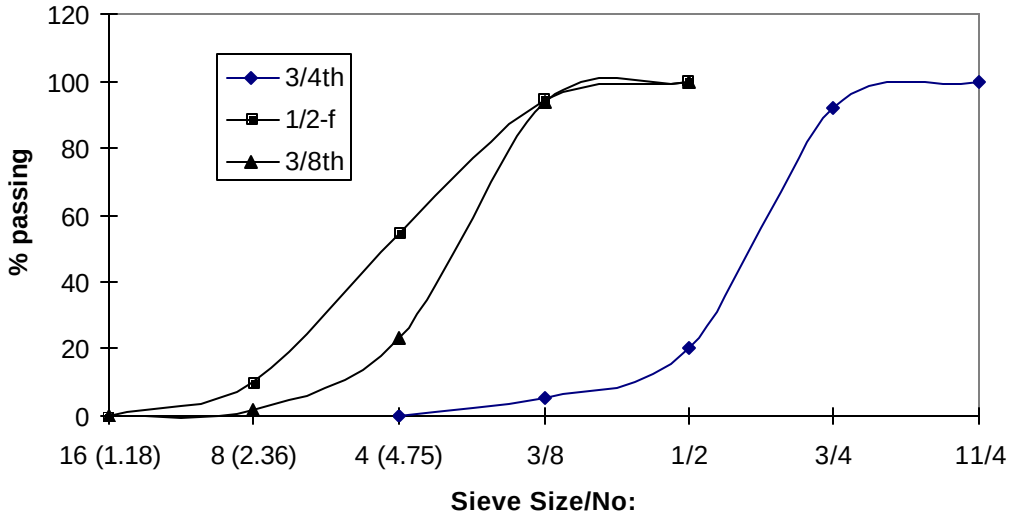

Figure 6: Gradation chart for coarse aggregate

Aggregates were then subjected to specific gravity tests, see ASTM C127 [10] and C128 [11] and AASHTO T84 and T85. A comparison of the densities of the coarse and fine aggregate was thus obtained, and as expected they are all almost identical.

Before making samples aggregates were placed in an oven overnight along with molds and hammer, and the oven was set to 325°F. Approximately two hours before mixing asphalt was also added to oven. Both the aggregates and asphalt were mixed together in metal bowl thoroughly before being placed in the compacting mold. Mixture was compacted by the 50 blows on both side of the specimen. After compaction was over each sample was allowed to cool in the mold before being taken out. The weight of each sample was carefully measured to calculate the mass density of the specimens as shown in Figure 7.

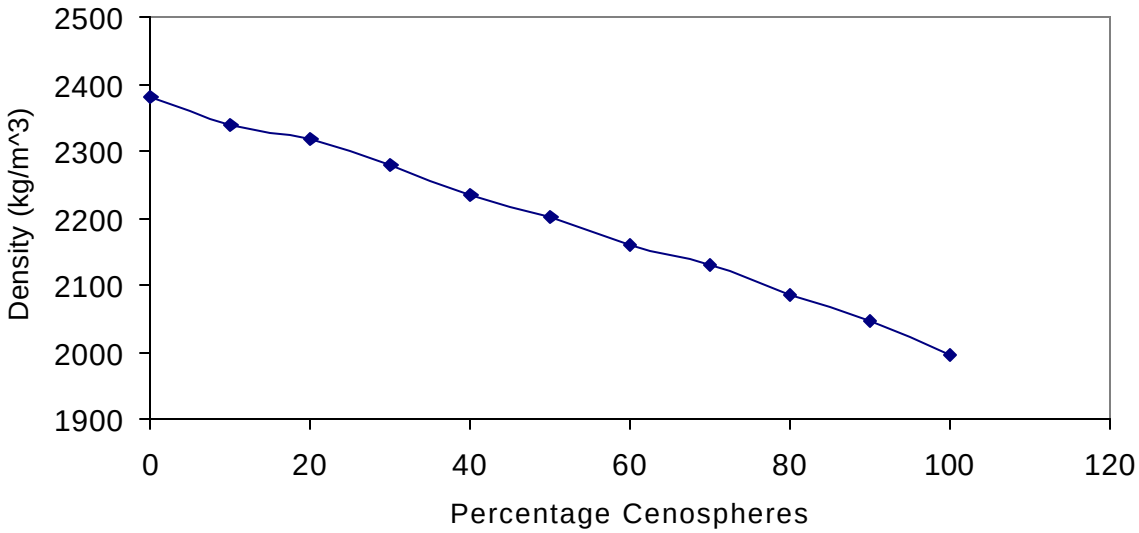

Figure 7: Change in mass density with percentage increase of cenospheres in Asphalt samples.

Bulk specific gravity test was performed on all the samples by measuring the saturated weights of the samples in air and water. Results show that there is not much variation in values of bulk specific gravity for specimens with different cenospheres content. (Figure 8).

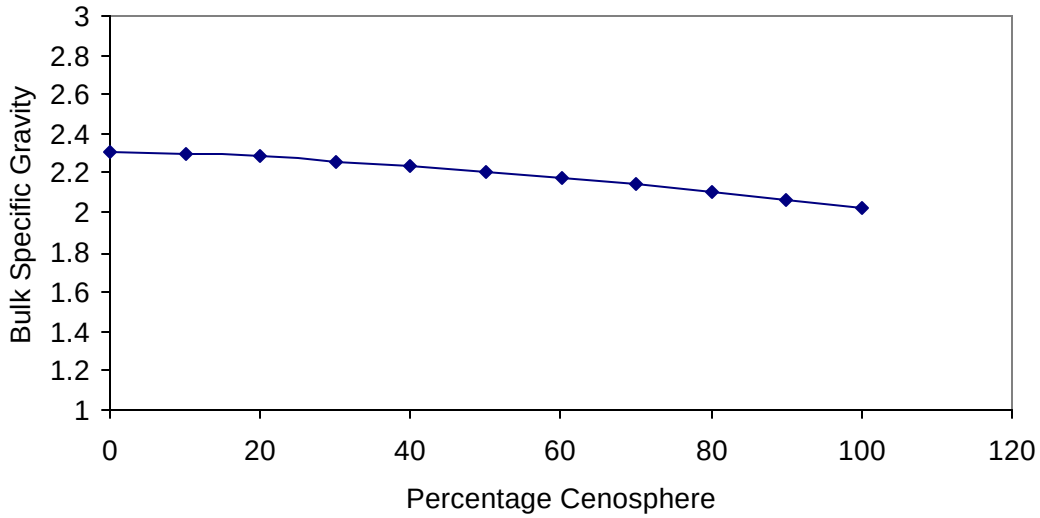

Figure 8: Change in Bulk Specific Gravity with percentage increase of cenospheres in Asphalt samples.

2.6 Results

Results obtained from the standing wave apparatus are applicable for sound incident normally to the surface of the sample and restrictions are placed on the use of the equipment to ensure that the theoretical conditions are closely approximate during the practical operation. Currently testing for acoustic properties of both Cement and Asphalt specimens is going on. Some of the results can be seen in Figures 9, 10 and 11. Each experiment has been performed five times to check the repeatability and to ensure the correct results.

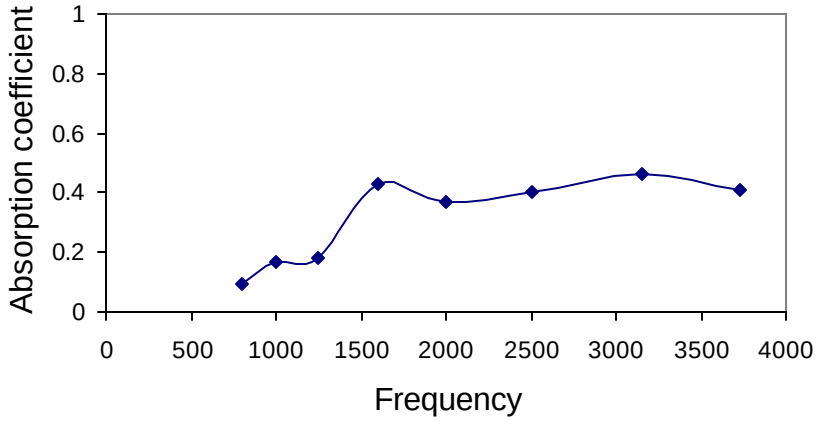

Figure 9: Variation of absorption coefficient as a function of frequency for two inch thick cement sample

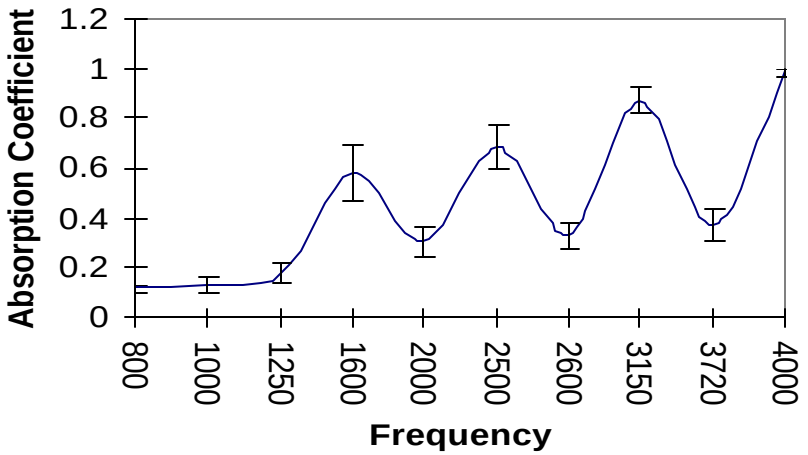

Figure 10: Variation of absorption coefficient as a function of frequency for two inch thick , 20% cenosphere sample

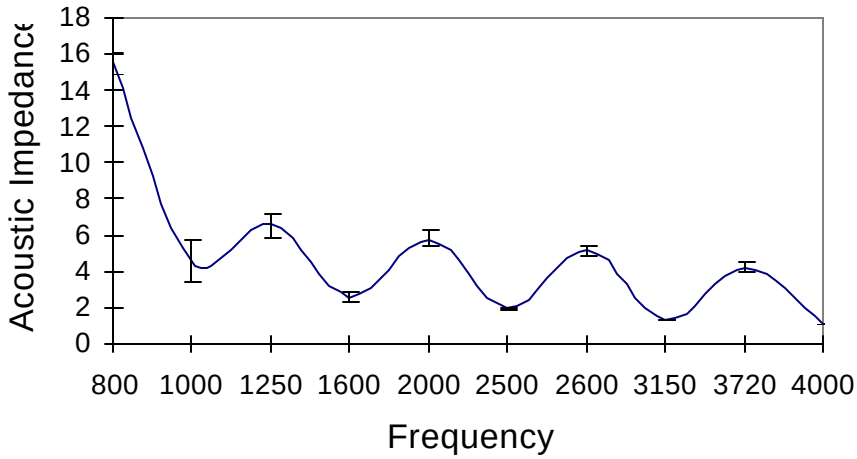

Figure 11: Acoustic impedance as a function of frequency for two inch, 20% cenosphere sample

2.7 Conclusions

Experimental studies on acoustical frequency response of cenosphere rich material are going on, results seem promising and will help in detailed understanding of their behaviors under different frequencies. Our initial results indicate that addition of cenospheres in cement increases its sound absorption properties. Also the test on mass density of both cement and Asphalt samples indicate appreciable reduction in density with increase in cenospheres content, where as there is not much change in the bulk specific gravity of Asphalt samples. The major accomplishment so far include establishing procedure to evaluate the acoustic properties, calibrating the test procedure and equipment. Further studies on the second year of the project will focus on the effect of particle distribution on the acoustic response of cement and asphalt in detail.

ACKNOWLEDGEMENTS

Financial support from the URI Transportation Research Center and the Rhode Island Department of Transportation is gratefully acknowledged.

REFERENCES

1. Utsuno, H., Tanaka, T., and Fujikawa, T., "Transfer Function Method For Measuring Characteristic Impedance and Propagation Constant of Porous Materials", *Journal of Acoustic Society of America*, Vol. 86, No.2, pp. 637, 1989.
2. Dunlop, J.I., "Specific Acoustic Impedance Measurement by a Protruding Tube Method", *Journal of Acoustic Society of America*, Vol.79, No.4, pp. 1177 - 1179, 1986.
3. Smith, C. D., and Parrot, T. L., "Comparison of Three Methods For Measuring Acoustic Properties of Bulk Materials", *Journal of Acoustic Society of America*, Vol.74, No.5, pp. 1577 – 1582, 1983.
4. Yamaguchi, M., Nakagawa, H., and Mizuno, T., "Sound Absorption Mechanism of Porous Asphalt Pavement", *Journal of Acoustic Society of Japan*, Vol. E, No. 20, pp. 29 – 43, 1999.
5. Meiarashi , S., and Ishida, M., "Improvement in the Effect of Drainage Asphalt Road Surface on Noise Reduction", *Journal. of Applied Acoustics*, Vol 47, No. 3, pp.189-204, 1996
6. Watts, G. R., Chandler-wilde, S.N., and Morgan, P.A., " The combined effects of porous asphalt surfacing and barriers on traffic noise", *Applied Acoustic*, Vol. 58, pp. 351 –377, 1999.
7. Watts, G. R., and Godfrey, N.S., " Effects on roadside noise levels of sound absorptive materials in noise barriers", *Applied Acoustic*, Vol. 58, pp. 385 –402, 1999.
8. "Standard test method for impedance and absorption of acoustical materials by the impedance tube method", *Annual Book of ASTM Standards*. Designation C384-98.
9. " Standard test method for sieve analysis of fine and coarse aggregates", *Annual Book of ASTM Standards*. Designation C136-01.
10. "Standard test method for specific gravity and absorption of coarse aggregate", *Annual Book of ASTM Standards*. Designation C127-88.
11. "Standard test method for specific gravity and absorption of fine aggregate", *Annual Book of ASTM Standards*. Designation C128-97.